Resource Scheduling for High-Capacity Multicast Service in Ultra-Dense LEO Satellite Networks

Ting Ma, *Member, IEEE*, Bo Qian, *Member, IEEE*, Xiaohan Qin, *Student Member, IEEE*, Xin Zhang, *Graduate Student Member, IEEE*, Lin X. Cai, *Senior Member, IEEE*, and Haibo Zhou, *Senior Member, IEEE*

***Abstract*—Ultra-dense low earth orbit (LEO) network has been envisioned as a promising solution to improve communication coverage and reliability. In this article, we investigate the resource scheduling for the downlink multigroup multicast cooperative transmissions in an ultra-dense LEO network, where multiple LEO satellites serve as aerial base stations to cooperatively offer high-capacity multicast service for ground users (GUs) within the coverage. To obtain the system max-min fair (MMF) capacity, we formulate a weighted MMF downlink beamforming and subchannel assignment problem. As the formulated problem is NP-hard and non-convex, we adopt a many-to-many matching model to solve the subchannel assignment, and apply the successive convex approximation (SCA) coupled with Gaussian randomization and cochannel power control to obtain the downlink beamforming during the matching process. Furthermore, the matching algorithm is guaranteed to converge to a two-side exchange stable matching within finite iteration steps. Extensive numerical results are provided to demonstrate the superiority and effectiveness of the proposed resource scheduling scheme for cooperative multicast transmissions.**

***Index Terms*—Resource scheduling, multicast, ultra-dense LEO networks, beamforming, subchannel assignment.**

I. Introduction

NOWADAYS, the ultra-dense low earth orbit (LEO) satellite network has attracted great attention from academia and industry owing to its vast and seamless coverage [1], [2], [3]. In 2015, SpaceX launched the Starlink satellite constellation project, which is composed of over 1600 satellites in mid-2021, and will eventually extend to nearly 12,000 low Earth orbit (LEO) satellites [4]. Hence, it is considered as a predictable and achievable paradigm in future communication networks to serve ground users (GUs) when the terrestrial communication system fails to work, such as in remote multicast service or other difficult-to-serve cases.

Recently, multicast transmission has been considered as an effective technology for the rising content-centric communication, such as video streaming, mobile TV and music streaming [5], [6], [7]. In content-centric communications, contents such as popular videos and TV programs can be multicast to multiple users to improve the transmission efficiency [6], [7], [8]. The multicast transmission is widely used in the following applications: news/sports/stock/weather update, distance education, teleconference, e-mail distribution, popular video distribution, etc. In the enhanced mobile broadband (eMBB) application of the fifth-generation (5 G) communication network, content-centric video streaming communications will have explosive demand. Hence, the multicast transmission has been considered as a promising technology in the future communication network.

When GUs requesting the same content are distributed in some rural areas or are far away from each other, the terrestrial communication system may not be able to efficiently provide multicast service due to the limited coverage. In these scenarios, a LEO satellite network is a promising solution to realize multicast transmissions for GUs. In an ultra-dense LEO network, there usually exist multiple LEO satellites simultaneously covering GUs. By employing cooperation among multiple satellites, a larger antenna array of more antennas is created, which can enhance the system performance [9], [10], [11]. Meanwhile, to meet the increasing demands for high capacity, strong robustness and low latency for communications, large-scale antenna arrays can be utilized at LEO satellites to achieve considerable array gains and enhance the multicast transmission performance [12]. When multiple LEO satellites equipped with multiple antennas providing multicast services, it is challenging to coordinate multiple antennas in different LEO satellites and implement resource scheduling for efficient multicast transmissions.

Facing these challenges, we first study subchannel partition for multigroup multicast cooperative transmissions in an ultra-dense LEO network. By appropriately allocating GUs in different subchannels, we can improve the multicast performance of GUs [13]. Since it is the worst receiving rate that determines the common information rate in multicast applications, we aim at maximizing the performance of the GU with the lowest rate

Manuscript received 27 February 2023; revised 6 June 2023; accepted 17 August 2023. Date of publication 6 September 2023; date of current version 13 February 2024. This work was supported in part by National Key R&D Program of China under Grant 2020YFB1806104, in part by Natural Science Fund for Distinguished Young Scholars of Jiangsu Province under Grant BK20220067, in part by National Natural Science Foundation Original Exploration Project of China under Grant 62250004, and in part by National Natural Science Foundation of China under Grant 62271244. The review of this article was coordinated by Prof. Giovanni GG Giambene. (*Corresponding author: Haibo Zhou*.)

Ting Ma, Xiaohan Qin, Xin Zhang, and Haibo Zhou are with the School of Electronic Science and Engineering, Nanjing University, Nanjing 210023, China (e-mail: majiawan27@163.com; xhderemail@smail.nju.edu.cn; zanxin@smail.nju.edu.cn; haibozhou@nju.edu.cn).

Bo Qian is with the Department of Mathematics and Theories, Peng Cheng Laboratory, Shenzhen 518000, China (e-mail: boqian@pcl.ac.cn).

Lin X. Cai is with the Department of Electrical and Computer Engineering, Illinois Institute of Technology, Chicago, IL 60616 USA (e-mail: lincai@iit.edu).

Digital Object Identifier 10.1109/TVT.2023.3312342

to narrow the rate gap among different GUs according to the classical max-min fairness (MMF) criterion [14], [15], [16]. Besides, a weighting factor is introduced to characterize the service levels of each GU [14], [15], [16]. For the GUs of the same service level, the weight factors are the same. In this article, we jointly optimize the weighted MMF downlink beamforming and subchannel assignment to maximize the minimum rate among all GUs in an ultra-dense LEO satellite network. We propose the subchannel assignment scheme by using a many-to-many matching model, and adopt the successive convex approximation (SCA) technology to obtain the beamforming vectors. Compared with previous works, the novelty and contributions of this article are highlighted as follows:

- *Cooperative multigroup multicast transmission:* We formulate a downlink multigroup multicast cooperative transmission problem in an ultra-dense LEO network, where the weighted MMF downlink beamforming and subchannel assignment are exploited. In this scenario, multiple LEO satellites equipped with multiple antennas provide multicast services for GUs under their coverage area.
- *Many-to-many matching model based subchannel assignment:* We adopt a many-to-many matching model to obtain the subchannel assignment. The matching algorithm can efficiently assign GUs with subchannels to maximize the lowest achievable rate among all GUs, and we show its convergence to a two-side exchange stable matching in finite iterations.
- *SCA based downlink beamforming:* In the process of matching, by combining the SCA with Gaussian randomization and cochannel power control, we propose an SCA based algorithm to efficiently obtain the downlink beamforming, which maximizes the performance of the GU with the lowest rate with convergence guarantee.

The remainder of this article is organized as follows. Section II reviews related works. Section III describes the system model of the multigroup multicast cooperative transmission in ultra-dense LEO networks, and formulates the weighted MMF downlink beamforming and subchannel assignment problem. In Sections IV and V, we provide the corresponding problem solution and simulation results, respectively. Section VI concludes the article and provides the future work.

II. Related Works

With the rapid development of smart mobile devices, wireless services expanded from traditional connection centric communication (e.g., telephone and e-mail, etc) to content-centric communication. In content-centric communications, the multicast transmission is envisioned as a promising solution for improving the system performance compared with the point-to-point transmission. The multicast service in content-centric communications has attracted growing interests during the last decades. In [14], N. Sidiropoulos et al. firstly studied the multicast beamforming for a single group of users. Then, in [15], N. Sidiropoulos et al. extended the multicast beamforming to multiple user groups, where two NP-hard optimization problems were formulated, i.e., minimizing transmit power under quality of service constraints and the power-constrained MMF problem, which were approximately solved by semi-definite relaxation, Gaussian randomization and the bisection method. Alternatively, in [17], M. Tao et al. presented a convex-concave procedure based algorithm to attain a stationary solution. However, when the problem scale grows, the computational complexity of traditional methods usually increase dramatically. Hence, new efficient beamforming algorithms need to be explored.

The multigroup multicast beamforming was developed in various scenarios, such as cloud radio access networks with wireless backhaul [16], intelligent reflecting surface aided wireless networks [18], massive multi-input and multi-output (MIMO) [19] and cloud-edge coordinated networks [20], etc. Another realistic application is found in the multibeam satellite communication systems [21], [22], [23]. Based on the state-of-the-art technologies in digital video broadcasting-satellite-second generation extension (DVB-S2X) of European Telecommunications Standards Institute (ETSI) [24], each spot beam of the satellite simultaneously serves multiple users by transmitting a single coded frame. This promising satellite communication system can well support the multigroup multicast transmissions, where different beams serve different groups of users [21]. Meanwhile, the satellite has been utilized as a complement of terrestrial base stations to increase the coverage in the next generation communication networks. Based on the 3 rd Generation Partnership Project (3GPP) [25], satellite radio access network (RAN) shall be supported for phase 2, and the corresponding support defined by the 3GPP will be considered in combination with RAN activities.

Recently, the multibeam satellite system has attracted numerous attention because of its pervasive coverage, high throughput and full frequency reuse across multiple narrow spot beams. Vahid Joroughi et al. [22] introduced a two-stage precoding design for multibeam multicast satellite systems, where the first stage is minimizing the inter-beam interference and the second stage is enhancing the intra-beam signal to interference plus noise ratio (SINR). Araniti et al. [26] investigated the multimedia content delivery for the emerging 5G-satellite networks. By dividing multicast terminals into different subgroups, a radio resource management algorithm was designed for multicast multimedia content transmissions, which can strike a tradeoff between user throughput and fairness. In [23], Li et al. investigated the outage constrained robust multigroup multicast beamforming for the multi-beam satellite communication via optimizing the outage SINR in the worst-case with full frequency reuse. In [27], Zheng et al. proposed a generic optimization framework for the joint multiuser linear precoding design in the forward link of fixed multibeam satellite systems, and further provided an iterative algorithm for the precoding vectors and power allocation strategy. Zhu et al. [6] investigated the downlink cooperative multigroup multicast transmissions in the integrated terrestrial-satellite network, where terrestrial base stations (BSs) and the satellite cooperatively offer multicast services for GUs by reusing the entire bandwidth.

Considering the large-scale nature of ultra-dense LEO networks, cooperative transmission of multiple LEO satellites can improve the transmission efficiency. In [9], by employing

III. System Model

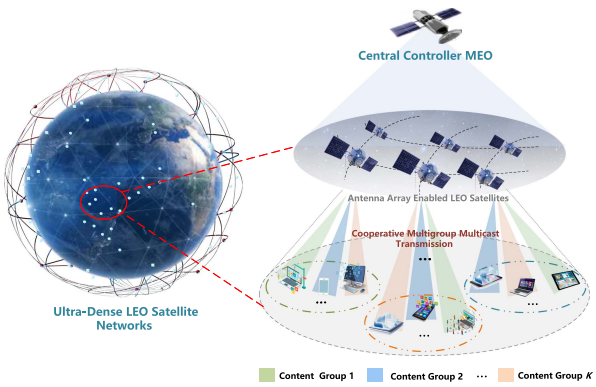

Fig. 1. Resource scheduling for multigroup multicast cooperative transmissions in an ultra-dense LEO network.

cooperation between the satellites, Röper et al. created an antenna array of more antennas to achieve high data rate communication. Abdelsadek et al. [10] designed a cell-free massive MIMO (CF-mMIMO) based LEO satellite network architecture with LEO satellites divided into clusters, where the power allocation and handover management is jointly optimized; In [11], Goto et al. presented a capacity analysis of MIMO LEO communication network, the BS achieves the service region through several LEO satellites.

The aforementioned works consider a single satellite, or use the entire bandwidth without subchannel division. In this article, we jointly study the large-scale antenna array enabled beamforming and subchannel assignment in an ultra-dense LEO satellite network with spectrum reuse and performance enhancement. We propose a low complexity algorithm for joint downlink beamforming and subchannel assignment for the cooperative multigroup multicast transmissions of multiple LEO satellites.

III. System Model

In Fig. 1, we investigate the downlink multigroup multicast cooperative high-capacity multicast transmission in ultra-dense LEO networks. Inspired by the two-layer satellite network [28], we introduce an medium earth orbit (MEO) satellite which covers these LEO satellites as a central controller to aggregate all information of LEO satellites and GUs, and manage the downlink multigroup multicast transmissions. The number and specific LEO satellites associated with the MEO is determined by positions of MEO and LEO satellites, together with the half-sided center angle of the MEO satellite. If the distance between the LEO and the MEO is smaller than the threshold distance that the LEO lies in the coverage of the MEO satellite, the LEO satellite is under the coverage of the MEO satellite. In a certain duration, the associated links between LEO satellites and GUs are assumed to remain unchanged, and thereby LEO satellites can keep providing multicast for GUs within a given region during an appointed time period. Meanwhile, owing to large scale of ultra-dense LEO networks, several LEO satellites can provide simultaneous coverage for GUs. By proper cooperation among these multiple LEO satellites, they can serve GUs in a cooperative manner to achieve better transmission performance. The number of LEO satellites involved in the cooperative transmission is determined by the number of LEO satellites which can simultaneously cover all GUs in a given region. When the given region is fixed, the situation of LEO satellites covering all GUs in the given region is unchanged during the appointed time period, and thereby the number of LEO satellites involved in the cooperation transmission is a constant. During a given time period, assume that there exist L LEO satellites cooperatively offering multicast services for a total of N GUs in their coverage. It should be noted that, due to the mobility of LEO satellites, after the appointed time period, if the situation of LEO satellites covering all GUs is changed, then the cooperation only occurs among the newest multiple LEO satellites covering all GUs, and the resource scheduling strategy will correspondingly update. Assuming that LEO satellite l is equipped with N_l antennas, $l \in \{1, \ldots, L\}$, then the total antenna number of LEO satellites can be calculated as $M = \sum_{l=1}^{L} N_l$. Assume that the channel state information (CSI) can be obtained for the LEO satellites. Then, the central controller MEO integrates all CSI via receiving CSI from LEO satellites. Since the CSI transmission from corresponding LEO satellites to MEO is via the inter orbital links (IOLs), the signalling latency is very small, which is determined by the light speed. Besides, based on [29], the position-related large-scale CSI can be obtained by satellites in an offline manner at a low cost. For the case of obtaining CSI offline, the delay associated with satellite communications will not affect the performance. Accordingly, referring to [6], [30], the perfect CSI knowledge is adopted. When the CSI changes a lot, the resource scheduling strategy will be correspondingly updated. In our setup, there are overall K contents that GUs can request, and each GU is equipped with a single antenna. Then, we partition GUs to K groups based on their requested content. Define the GU group $\mathcal{G}_k = \{\mathcal{U}_{1,k}, \ldots, \mathcal{U}_{G_k,k}\}$ as GUs that request content k, where G_k is denoted by the number of GUs in $\mathcal{G}_k$, i.e., $G_k = |\mathcal{G}_k|$, $k \in \{1, \ldots, K\}$. In this article, we suppose that a certain GU requests only one content at a given time. Therefore, $\mathcal{G}_k \bigcap \mathcal{G}_j = \emptyset$ for $k \neq j$ and $\sum_{k=1}^{K} G_k = N$. Important notations are listed in Table I.

When LEO satellites with a total of M antennas multicast contents for K GU groups, each GU will simultaneously receive the signals from M LEO satellites, which includes the desired signal and interference signals from LEO satellites. To reduce interference and improve the performance, the total bandwidth B_{tol} is partitioned into H subchannels. GUs in the same group will use one or multiple subchannels for the transmissions, and one subchannel can match with multiple GU groups. Let $\boldsymbol{X} = \{x_{k,h}\} \in \mathbb{R}^{K \times H}$ be the subchannel assignment matrix with $x_{k,h} = \{0, 1\}$, where $x_{k,h} = 1$ means that group $\mathcal{G}_k$ is served by LEO satellites over c_h and $x_{k,h} = 0$ otherwise. Subsequently, we express the transmit signal of LEO on c_h as

$$\boldsymbol{x}_h = \sum_{k=1}^{K} \boldsymbol{w}_{k,h} x_{k,h} s_k, \tag{1}$$

where $s_k \in \mathbb{C}$ represents the transmit signal for $\mathcal{G}_k$ satisfying $\mathbb{E}[|s_k|^2] = 1$, and $\boldsymbol{w}_{k,h} \in \mathbb{C}^M$ is the beamforming of $\mathcal{G}_k$ over c_h. Here $\boldsymbol{w}_{k,h}$ is the aggregation beamforming vector of all L

TABLE I
MAIN NOTATIONS

Notation	Description
L	The number of LEO satellites
N_l	The number of antennas equipped with LEO l
N	The number of GUs
M	The total number of antennas equipped with LEO satellites
B_{tol}	The total bandwidth of LEO satellites
H	The number of subchannels
B_h	Bandwidth allocated in c_h
K	The number of GU groups (contents)
$\mathcal{G}_k$	Set of GUs requesting content k
$\mathcal{U}_{i,j}$	The i-th GU in $\mathcal{G}_k$
G_k	The number of GUs in $\mathcal{G}_k$
$\mathcal{G}$	Set of all K GU groups
$\mathcal{C}$	Set of all H subchannels
c_h	The h-th subchannel
$\boldsymbol{g}_{i,j,h}$	Channel gain from LEO to $\mathcal{U}_{i,j}$ over c_h
s_k	Transmit signal for $\mathcal{G}_k$
$\boldsymbol{w}_{k,h}$	Beamforming for $\mathcal{G}_k$ over c_h
$\boldsymbol{X}$	Subchannel assignment matrix
$y_{i,j,h}$	Received signal of $\mathcal{U}_{i,j}$ over c_h
$n_{i,j,h}$	Additive white Gaussian noise (AWGN)
$\gamma_{i,k,n}$	Received SINR of $\mathcal{U}_{i,j}$ over c_h
P_l	Maximum power of LEO l
$R_{i,j}$	Achievable rate of $\mathcal{U}_{i,j}$
$R^0_{i,j}$	Prescribed target achievable rate of $\mathcal{U}_{i,j}$

LEO satellites with M antennas. That is, we can express $\boldsymbol{w}_{k,h}$ as $\boldsymbol{w}_{k,h} = [\boldsymbol{w}^1_{k,h}; \cdots; \boldsymbol{w}^L_{k,h}]$, where $\boldsymbol{w}^l_{k,h} \in \mathbb{C}^{N_l}$ represents the beamforming vector of LEO satellite l. Therefore, for given aggregation beamforming vector of all LEO satellites, we can derive the corresponding beamforming vector of LEO l

$$\boldsymbol{w}^l_{k,h} = \boldsymbol{A}_l \boldsymbol{w}_{k,h},$$

where

$$\begin{aligned} &\boldsymbol{A}_l = [\boldsymbol{B}_1, \ldots, \boldsymbol{B}_L] \in \mathbb{R}^{N_l \times M}, \\ &\boldsymbol{B}_l = \boldsymbol{I}_{N_l},\ \boldsymbol{B}_{l'} = \boldsymbol{0}_{N_l \times N_{l'}},\ l' \neq l, \end{aligned} \tag{2}$$

with $\boldsymbol{I}_{N_l}$ being the N_l dimensional identity matrix, and $\boldsymbol{0}_{N_l \times N_{l'}}$ is a zero matrix with dimension $N_l \times N_{l'}$. Notice that, for GUs requesting the same content but lying in different areas, it is better to cover them with different beams. However, we can combine the beamforming vectors of GUs that request the same content. Hence, in (1), we consider only one beamforming vector for each group using the same subchannel. Assume that the waveforms are uncorrelated with each other, we formulate the transmit power of LEO satellite l as

$$\sum_{h=1}^{H} \sum_{k=1}^{K} \|\boldsymbol{A}_l \boldsymbol{w}_{k,h}\|^2 \tag{3}$$

with $\boldsymbol{A}_l$ is defined in (2).

The received signal of $\mathcal{U}_{i,j}$ over c_h can be expressed as

$$y_{i,j,h} = \boldsymbol{g}^{\mathrm{H}}_{i,j,h} \boldsymbol{x}_h + n_{i,j,h} \tag{4}$$

$$= \boldsymbol{g}^{\mathrm{H}}_{i,j,h} \boldsymbol{w}_{j,h} x_{j,h} s_j + \boldsymbol{g}^{\mathrm{H}}_{i,j,h} \sum_{k=1, k\neq j}^{K} \boldsymbol{w}_{k,h} x_{k,h} s_k + n_{i,j,h}, \tag{5}$$

in which $\boldsymbol{g}_{i,j,h}$ denotes the M-dimensional channel vector from LEO to $\mathcal{U}_{i,j}$ over c_h, and $n_{i,j,h}$ represents the AWGN with variances $\sigma^2_{i,j,h}$. In this article, we generate the channel vector $\boldsymbol{g}_{i,j,h}$ as in [31], which is given by

$$\boldsymbol{g} = \sqrt{C_{loss}} \xi^{\frac{1}{2}} e^{-j\phi} \boldsymbol{b}^{\frac{1}{2}}, \tag{6}$$

where $C_{loss} = \left(\frac{\lambda}{4\pi R}\right)^2$ is the free-space path loss coefficient with λ being the wave length of transmission signal and R being the distance between GU and LEO, ξ represents the power attenuation of the rain fading, $\phi \sim [0, 2\pi]$ denotes the phase of the antenna feeds, and $\boldsymbol{b}$ is the beam gain. According to [27], we set each element of $\boldsymbol{b}$ as

$$b = \left(\frac{J_1(u)}{2\,u} + 36\frac{J_3(u)}{u^3}\right)^2, \tag{7}$$

in which $u = 2.07123 \sin\theta / \sin\theta_{3\,\mathrm{dB}}$, θ denotes the angle between the spot beam center and the receiver GU's position from the LEO satellite, $\theta_{3\,\mathrm{dB}}$ is the 3-dB angle for the beam, and J_1 and J_3 are the first order Bessel function of first-kind and the third order Bessel function of first-kind, respectively.

Notice that, the first term of (5) is the expected signal for $\mathcal{U}_{i,j}$, while the second term is the suffered inter-group co-channel interference. Subsequently, we formulate the received SINR of $\mathcal{U}_{i,j}$ over c_h as

$$\gamma_{i,j,h} = \frac{x_{j,h} |\boldsymbol{g}^{\mathrm{H}}_{i,j,h} \boldsymbol{w}_{j,h}|^2}{\sum_{k=1,k\neq j}^{K} x_{k,h} |\boldsymbol{g}^{\mathrm{H}}_{i,j,h} \boldsymbol{w}_{k,h}|^2 + \sigma^2_{i,j,h}}. \tag{8}$$

where $\sigma^2_{i,j,h}$ is the AWGN power. We can observe from (8) that, $x_{j,h} = 0$ indicates $\gamma_{i,j,h} = 0$. By combining signals of all subchannels, the achievable rate of $\mathcal{U}_{i,j}$ is

$$R_{i,j} = \sum_{h=1}^{H} B_h \log\left(1 + \gamma_{i,j,h}\right), \tag{9}$$

where B_h is the bandwidth allocated to subchannel c_h with satisfying $\sum_{h=1}^{H} B_h = B_{tol}$.

Since there exists inter-group co-channel interference in the cooperative downlink multigroup multicast transmission, it is of great significance to construct the optimal subchannel assignment $\boldsymbol{X}$ and beamforming vectors $\boldsymbol{w}$ to achieve the best system performance. The multicast transmission performance is determined by the lowest achievable rate among all GUs, and thus our objective is to maximize the minimum achievable rate of the GUs, referred to as MMF criterion in [14], [15], [16]. Meanwhile, taking into account different service levels for individual GU, we consider a prescribed constant weight factor $1/R^0_{i,j}$, where $R^0_{i,j}$ is a predetermined target achievable rate of GU $\mathcal{U}_{i,j}$. Consequently, we aim at finding the optimal subchannel assignment and beamforming design to maximize the worst weighted achievable rate among all GUs, i.e., solving the following weighted MMF problem

$$(\mathcal{F}) \max_{\{\boldsymbol{w}_{j,h}\}, \boldsymbol{X}} \min_{j\in\{1,\ldots,K\}} \min_{i\in[1,G_j]} \frac{1}{R^0_{i,j}} R_{i,j} \tag{10}$$

$$\text{s.t.} \sum_{h=1}^{H} \sum_{j=1}^{K} x_{j,h} \|\boldsymbol{A}_l \boldsymbol{w}_{j,h}\|^2 \leqslant P_l,\ l \leqslant L, \tag{10a}$$

$$x_{j,h} \in \{0,1\},\ j \leqslant K,\ h \leqslant H, \tag{10b}$$

$$\sum_{h=1}^{H} x_{j,h} \geqslant 1,\ j \leqslant K, \tag{10c}$$

where $R_{i,j}$ is the achievable rate of GU $\mathcal{U}_{i,j}$ defined in (9), the term $\min_{j\in\{1,\ldots,K\}} \min_{i\in[1,G_j]} \frac{1}{R^0_{i,j}} R_{i,j}$ in the objective function is the minimum weighted achievable rate among all GUs, constraint (10a) represents the transmit power constraint with $\boldsymbol{A}_l$ given by (2) and P_l being the maximum transmit power of LEO l, constraint (10b) defines the subchannel selection binary variable, and constraint (10c) implies that at least one subchannel should be assigned to each group. It should be noted that, since there are multiple GU groups and multiple GUs in each GU group, the worst weighted achievable rate in problem $(\mathcal{F})$ can be presented by two minimizations. Specifically, the inner minimization is to find the minimum weighted achievable rate in each GU group, i.e., $\min_{i\in[1,G_j]} \frac{1}{R^0_{i,j}} R_{i,j}, \forall\, j$, while the outer minimization is to find the minimum weighted achievable rate among all groups.

When measuring the system performance, we introduce capacity of GU group $\mathcal{G}_k$ and system capacity as

$$C_j = \min_{i\in[1,G_j]} R_{i,j} \text{ and } C = \min_{j\in\{1,\ldots,K\}} \min_{i\in[1,G_j]} \frac{1}{R^0_{i,j}} R_{i,j},$$

respectively. Via solving problem $(\mathcal{F})$, we can obtain the optimal subchannel assignment matrix $\boldsymbol{X}$ and beamforming vectors $\boldsymbol{w}$ to maximize the system capacity with LEO satellite power constraints, where the maximum system capacity is referred to as the system MMF capacity.

Notice that, in the particular case of $\boldsymbol{X} = [1,\ldots,1]'$ and $H = 1$, problem $(\mathcal{F})$ has been proven to be NP-hard in [15]. Therefore, we can immediately deduce that Problem $(\mathcal{F})$ is an NP-hard problem, which is usually difficult to solve.

IV. Algorithm Design for the Weighted MMF Problem

In this section, we attempt to seek efficient solutions for the weighted MMF problem $(\mathcal{F})$, where the downlink beamforming $\boldsymbol{w}$ and the subchannel assignment $\boldsymbol{X}$ are coupled. First, for a fixed subchannel assignment $\boldsymbol{X}$, we discuss how to obtain the beamforming $\boldsymbol{w}$ with the aid of the SCA technology. Then, we use a matching game to determine the subchannel assignment $\boldsymbol{X}$.

A. Multicast Beamforming Algorithm

With a fixed subchannel assignment $\boldsymbol{X}$, we can reduce problem $(\mathcal{F})$ to

$$(\mathcal{F}_w) \max_{\{\boldsymbol{w}_{j,h}\}} \min_{j\in\{1,\ldots,K\}} \min_{i\in[1,G_j]} \frac{1}{R^0_{i,j}} R_{i,j}$$
$$\text{s.t.} \sum_{h=1}^{H}\sum_{j=1}^{K} x_{j,h}\|\boldsymbol{A}_l\boldsymbol{w}_{j,h}\|^2 \leqslant P_l,\ \forall\, l. \tag{11}$$

By introducing an auxiliary variable $t > 0$, problem $(\mathcal{F}_w)$ can be equivalently converted to

$$(\mathcal{F}_w) \max_{\{\boldsymbol{w}_{j,h}\},t} t \tag{12}$$
$$\text{s.t.} \ \frac{1}{R^0_{i,j}} R_{i,j} \geqslant t,\ \forall\, i,\ j, \tag{12a}$$
$$\sum_{h=1}^{H}\sum_{j=1}^{K} x_{j,h}\|\boldsymbol{A}_l\boldsymbol{w}_{j,h}\|^2 \leqslant P_l,\ \forall\, l. \tag{12b}$$

Obviously, the non-convex problem $(\mathcal{F}_w)$ is still NP-hard. In the sequel, approximations will be made on $R_{i,j}$ to convert problem $(\mathcal{F}_w)$ to a convex programming based on the SCA technology.

To begin with, we will transform the vector variables in problem $(\mathcal{F}_w)$ into matrix variables. Note that, the following two terms in problem $(\mathcal{F}_w)$ can be rewritten as

$$\begin{aligned}\|\boldsymbol{w}_{j,h}\|^2 &= \mathrm{tr}\left(\boldsymbol{w}^{\mathrm{H}}_{j,h}\boldsymbol{w}_{j,h}\right) = \mathrm{tr}\left(\boldsymbol{w}_{j,h}\boldsymbol{w}^{\mathrm{H}}_{j,h}\right),\\ \left|\boldsymbol{g}^{\mathrm{H}}_{i,j,h}\boldsymbol{w}_{j,h}\right|^2 &= \mathrm{tr}\left(\boldsymbol{w}^{\mathrm{H}}_{j,h}\boldsymbol{g}_{i,j,h}\boldsymbol{g}^{\mathrm{H}}_{i,j,h}\boldsymbol{w}_{j,h}\right)\\ &= \mathrm{tr}\left(\boldsymbol{g}_{i,j,h}\boldsymbol{g}^{\mathrm{H}}_{i,j,h}\boldsymbol{w}_{j,h}\boldsymbol{w}^{\mathrm{H}}_{j,h}\right),\end{aligned} \tag{13}$$

in which $\mathrm{tr}(\cdot)$ represents the trace of a matrix. For concise presentation, we introduce the following notations,

$$\begin{aligned}\boldsymbol{w}_h &= (\boldsymbol{w}_{1,h};\cdots;\boldsymbol{w}_{K,h}) \in \mathbb{C}^{KM},\\ \boldsymbol{W}_h &= \boldsymbol{w}_h\boldsymbol{w}^{\mathrm{H}}_h \in \mathbb{C}^{KM\times KM},\\ \hat{\boldsymbol{Q}}_{i,j,h} &= \boldsymbol{g}_{i,j,h}\boldsymbol{g}^{\mathrm{H}}_{i,j,h} \in \mathbb{C}^{M\times M},\\ \boldsymbol{Q}_{k;i,j,h} &= \mathbf{Blk}\{\boldsymbol{0},\cdots,\boldsymbol{0},\hat{\boldsymbol{Q}}_{i,j,h},\boldsymbol{0},\cdots,\boldsymbol{0}\} \in \mathbb{C}^{KM\times KM},\end{aligned} \tag{14}$$

in which $\mathbf{Blk}\{\cdot\}$ represents the block diagonalization, the k-th block of $\boldsymbol{Q}_{k;i,j,h}$ is $\hat{\boldsymbol{Q}}_{i,j,h}$, and others are M-dimensional zero matrices. By substituting these notations in problem $(\mathcal{F}_w)$, we can obtain the equivalent problem as follows

$$(\hat{\mathcal{F}}_W) \max_{\{\boldsymbol{W}_h\},t} t \tag{15}$$
$$\text{s.t.} \ \frac{1}{R^0_{i,j}} \hat{R}_{i,j} \geqslant t,\ \forall\, i,\ j, \tag{15a}$$
$$\sum_{h=1}^{H} \mathrm{tr}(\boldsymbol{C}_{h,l}\boldsymbol{W}_h) \leqslant P_l,\ \forall\, l, \tag{15b}$$
$$\mathrm{rank}(\boldsymbol{W}_h) = 1, \boldsymbol{W}_h \succcurlyeq \boldsymbol{0},\ \forall\, h, \tag{15c}$$

where

$$\hat{R}_{i,j} = \sum_{h=1}^{H} B_h \log\left(1 + \frac{x_{j,h}\mathrm{tr}(\boldsymbol{Q}_{j;i,j,h}\boldsymbol{W}_h)}{\sum_{k=1,k\neq j}^{K} x_{k,h}\mathrm{tr}(\boldsymbol{Q}_{k;i,j,h}\boldsymbol{W}_h) + \sigma^2_{i,j,h}}\right), \tag{16}$$

and

$$\boldsymbol{C}_{h,l} = D\left\{x_{1,h}\boldsymbol{A}^{\mathrm{T}}_l\boldsymbol{A}_l,\ldots,x_{K,h}\boldsymbol{A}^{\mathrm{T}}_l\boldsymbol{A}_l\right\} \in \mathbb{C}^{KM\times KM},$$

with $\boldsymbol{A}_l$ is given by (2).

Since the non-convex rank-1 constraint (15c) is difficult to handle, referring to [6], [14], [15], we first remove the rank-1

constraint to obtain the following relaxed MMF problem

$$(\hat{\mathcal{F}}_r) \quad \max_{\{\boldsymbol{W}_h\},t} \quad t \tag{17}$$

$$\text{s.t.} \quad \frac{1}{R^0_{i,j}}\hat{R}_{i,j} \geqslant t,\ \forall\, i,\ j, \tag{17a}$$

$$\sum_{h=1}^{H} \mathrm{tr}(\boldsymbol{C}_{h,l}\boldsymbol{W}_h) \leqslant P_l,\ \forall\, l, \tag{17b}$$

and then recover the beamforming vector $\boldsymbol{w}_h$. Since constraint (17a) is still non-convex due to the nonconcavity of $\hat{R}_{i,j}$, we will further approximate $\hat{R}_{i,j}$.

Before going on, we give the SCA result in the matrix form based on the SCA technology of Proposition B.3 in [32].

Lemma 1: For a convex function $f(\boldsymbol{W})$ of matrix $\boldsymbol{W}$, it holds

$$f(\boldsymbol{W}) \geqslant f(\tilde{\boldsymbol{W}}) + \mathrm{tr}[\nabla f(\tilde{\boldsymbol{W}})^{\mathrm{H}}(\boldsymbol{W} - \tilde{\boldsymbol{W}})], \tag{18}$$

where $\nabla f(\cdot)$ is the first order derivative of $f(\cdot)$, and $\tilde{\boldsymbol{W}}$ is a arbitrarily given matrix.

Now we are in position to give the following theorem about the approximation on $\hat{R}_{i,j}$.

Theorem 1: For an arbitrarily given matrix $\bar{\boldsymbol{W}}_h \in \mathbb{C}^{KM\times KM}$, the term $\bar{R}_{i,j}$ in (17a) has a lower bound of

$$\bar{R}_{i,j} = \sum_{h=1}^{H} B_h \left\{ \log\left(\mathrm{tr}\left[\sum_{k=1}^{K} x_{k,h}\boldsymbol{Q}_{k;i,j,h}\boldsymbol{W}_h\right] + \sigma^2_{i,j,h}\right) - \log\left(\mathrm{tr}\left[\sum_{k=1,k\neq j}^{K} x_{k,h}\boldsymbol{Q}_{k;i,j,h}\bar{\boldsymbol{W}}_h\right] + \sigma^2_{i,j,h}\right) - \frac{(\log e)\sum_{k=1,k\neq j}^{K} x_{k,h}\mathrm{tr}[\boldsymbol{Q}_{k;i,j,h}(\boldsymbol{W}_h - \bar{\boldsymbol{W}}_h)]}{\mathrm{tr}\left[\sum_{k=1,k\neq j}^{K} x_{k,h}\boldsymbol{Q}_{k;i,j,h}\bar{\boldsymbol{W}}_h\right] + \sigma^2_{i,j,h}} \right\}. \tag{19}$$

Furthermore, $\bar{R}_{i,j}$ is a concave function of $\boldsymbol{W}_h$, and $\bar{R}_{i,j} = \hat{R}_{i,j}$ if $\bar{\boldsymbol{W}}_h = \boldsymbol{W}_h$.

Proof: First, we can rewrite

$$\hat{R}_{i,j} = \sum_{h=1}^{H} B_h \left[\log\left(\mathrm{tr}\left[\sum_{k=1}^{K} x_{k,h}\boldsymbol{Q}_{k;i,j,h}\boldsymbol{W}_h\right] + \sigma^2_{i,j,h}\right) - \log\left(\mathrm{tr}\left[\sum_{k=1,k\neq j}^{K} x_{k,h}\boldsymbol{Q}_{k;i,j,h}\boldsymbol{W}_h\right] + \sigma^2_{i,j,h}\right)\right]. \tag{20}$$

Notably, for arbitrary i, j, h, functions

$$f_1(\boldsymbol{W}_h) = \log\left(\mathrm{tr}\left[\sum_{k=1}^{K} x_{k,h}\boldsymbol{Q}_{k;i,j,h}\boldsymbol{W}_h\right] + \sigma^2_{i,j,h}\right)$$

and

$$f_2(\boldsymbol{W}_h) = \log\left(\mathrm{tr}\left[\sum_{k=1,k\neq j}^{K} x_{k,h}\boldsymbol{Q}_{k;i,j,h}\boldsymbol{W}_h\right] + \sigma^2_{i,j,h}\right)$$

are concave with respect to $\boldsymbol{W}_h$. Then, on basis of Lemma 1, for an arbitrarily given matrix $\bar{\boldsymbol{W}}_h$, it holds

$$f_2(\boldsymbol{W}_h) \leqslant f_2(\bar{\boldsymbol{W}}_h) + \mathrm{tr}[\nabla f_2(\bar{\boldsymbol{W}}_h)^{\mathrm{T}}(\boldsymbol{W}_h - \bar{\boldsymbol{W}}_h)], \tag{21}$$

where $\nabla f_2(\cdot)$ is the first order derivative of $f_2(\cdot)$. With the relationships

$$\frac{\partial \log(x)}{\partial x} = \frac{1}{x} \quad \text{and} \quad \frac{\partial \mathrm{tr}(\boldsymbol{A}\boldsymbol{X})}{\partial \boldsymbol{X}} = \boldsymbol{A}^{\mathrm{T}},$$

we can deduce

$$\nabla f_2(\bar{\boldsymbol{W}}_h) = \frac{(\log e)\sum_{k=1,k\neq j}^{K} x_{k,h}\boldsymbol{Q}^{\mathrm{T}}_{k;i,j,h}}{\mathrm{tr}\left[\sum_{k=1,k\neq j}^{K} x_{k,h}\boldsymbol{Q}_{k;i,j,h}\bar{\boldsymbol{W}}_h\right] + \sigma^2_{i,j,h}}. \tag{22}$$

Consequently, it holds $\hat{R}_{i,j} \geqslant \bar{R}_{i,j}$ with $\bar{R}_{i,j}$ defined in (19). In particular, $\bar{R}_{i,j}$ is concave, and we have $\hat{R}_{i,j} = \bar{R}_{i,j}$ when $\bar{\boldsymbol{W}}_h = \boldsymbol{W}_h$.

By substituting $\hat{R}_{i,j}$ in (17a) by $\bar{R}_{i,j}$, we can approximately convert problem $(\hat{\mathcal{F}}_r)$ to the following problem

$$(\mathcal{F}_r) \quad \max_{\{\boldsymbol{W}_h\},t} \quad t \tag{23}$$

$$\text{s.t.} \quad \frac{1}{R^0_{i,j}}\bar{R}_{i,j} \geqslant t,\ \forall\, i,\ j, \tag{23a}$$

$$\sum_{h=1}^{H} \mathrm{tr}(\boldsymbol{C}_{h,l}\boldsymbol{W}_h) \leqslant P_l,\ \forall\, l, \tag{23b}$$

$$\boldsymbol{W}_h \geqslant \boldsymbol{0},\ \forall\, h. \tag{23c}$$

According to Theorem 1, we can deduce that constraint (23a) is convex. Particularly, constraint set (23a) is a convex set included in the constraint set (17a), which implies that the optimal objective value of problem $(\mathcal{F}_r)$ is a lower bound of that of problem $(\hat{\mathcal{F}}_r)$. Obviously, problem $(\mathcal{F}_r)$ is convex with respect to $\boldsymbol{W}_h$. Hence we can solve it by convex solvers such as CVX [33]. Through multiple iterations of solving problem $(\mathcal{F}_r)$, we can obtain a local minimum or a saddle point of problem $(\hat{\mathcal{F}}_r)$ with a feasible starting point [34].

Based on the above arguments, we obtain a solution $\boldsymbol{W}_h$ to problem $(\hat{\mathcal{F}}_r)$. When the obtained solution $\boldsymbol{W}_h$, $h = 1, \ldots, H$, are all matrices with rank-1, it is not difficult to use the eigenvalue decomposition to get the corresponding beamforming vector. However, since problem $(\mathcal{F}_r)$ is a relaxed problem without rank-1 constraints, the rank of derived $\boldsymbol{W}_h$ is usually larger than 1. For this case, we utilize the Gaussian randomization method presented in [14], [35], [36] to produce candidate beamforming vectors. To be specific, via using the eigenvalue decomposition $\boldsymbol{W}_h = \boldsymbol{U}_h\boldsymbol{\Sigma}_h\boldsymbol{U}^{\mathrm{H}}_h$, we generate the beamforming vector on sub-channel c_h as $\boldsymbol{w}_h = \boldsymbol{U}_h\boldsymbol{\Sigma}_h^{\frac{1}{2}}\boldsymbol{\varphi}_h$, where $\boldsymbol{\varphi}_h \sim CN(\boldsymbol{0}, \boldsymbol{I})$ represents a vector of zero-mean, unit variance, uncorrelated Gaussian random variables. It is straightforward to see $\mathbb{E}[\boldsymbol{w}_h\boldsymbol{w}^{\mathrm{H}}_h] = \boldsymbol{W}_h$.

Notice that, when generating candidate beamforming vectors by the Gaussian randomization, the power constraint (12b) on the beamforming vector may not be satisfied. Hence, it is possible that the satellite power is not used up or the power constraint (12b) is not satisfied. To avoid these two cases, similar to [6],

[14], [15], we further formulate the power scaling problem to acquire the optimal power scaling factors $p_{j,h}$ on basis of the obtained beamforming vectors, which is given by

$$(\hat{\mathcal{F}}_p) \max_{\{p_{j,h}\},t} \quad t \tag{24}$$

$$\text{s.t.} \sum_{h=1}^{H} B_h \log\left(1+\frac{x_{j,h}p_{j,h}|\boldsymbol{g}_{i,j,h}^{\mathrm{H}}\boldsymbol{w}_{j,h}|^2}{\sum_{k=1,k\neq j}^{K} x_{k,h}p_{k,h}|\boldsymbol{g}_{i,j,h}^{\mathrm{H}}\boldsymbol{w}_{k,h}|^2+\sigma_{i,j,h}^2}\right) \geqslant tR_{i,j}^0,\ \forall i,\ j, \tag{24a}$$

$$\sum_{h=1}^{H}\sum_{j=1}^{K} x_{j,h}p_{j,h}\|\boldsymbol{A}_l\boldsymbol{w}_{j,h}\|^2 \leqslant P_l,\ \forall l, \tag{24b}$$

$$p_{j,h} \geqslant 0,\ \forall j,\ h. \tag{24c}$$

Problem $(\hat{\mathcal{F}}_p)$ is not convex due to the nonconvexity of constraint (24a). Thus, we will approximately convert constraint (24a) to a convex one in the following.

With introducing the matrix variable $\boldsymbol{P}=\{p_{j,h}\}\in\mathbb{C}^{K\times H}$, we denote

$$g_1^{ij}(\boldsymbol{P}) \triangleq \sum_{h=1}^{H} B_h \log\left(1+\frac{x_{j,h}p_{j,h}|\boldsymbol{g}_{i,j,h}^{\mathrm{H}}\boldsymbol{w}_{j,h}|^2}{\sum_{k=1,k\neq j}^{K} x_{k,h}p_{k,h}|\boldsymbol{g}_{i,j,h}^{\mathrm{H}}\boldsymbol{w}_{k,h}|^2+\sigma_{i,j,h}^2}\right). \tag{25}$$

It is straightforward to rewrite $g_1^{ij}(\boldsymbol{P})$ as

$$g_1^{ij}(\boldsymbol{P}) = \sum_{h=1}^{H} B_h \log\left(\sum_{k=1}^{K} x_{k,h}p_{k,h}|\boldsymbol{g}_{i,j,h}^{\mathrm{H}}\boldsymbol{w}_{k,h}|^2+\sigma_{i,j,h}^2\right) - g_2^{ij}(\boldsymbol{P}), \tag{26}$$

with

$$g_2^{ij}(\boldsymbol{P}) \triangleq \sum_{h=1}^{H} B_h \log\left(\sum_{k=1,k\neq j}^{K} x_{k,h}p_{k,h}|\boldsymbol{g}_{i,j,h}^{\mathrm{H}}\boldsymbol{w}_{k,h}|^2+\sigma_{i,j,h}^2\right). \tag{27}$$

We can observe that, both function $g_2^{ij}(\boldsymbol{P})$ and the first term in function $g_1^{ij}(\boldsymbol{P})$ are concave with respect to $\boldsymbol{P}$, but $g_1^{ij}(\boldsymbol{P})$ is not a concave function. Therefore, we provide the following theorem to approximately transform the nonconcave function $g_1^{ij}(\boldsymbol{P})$ into a concave one.

Theorem 2: Function $g_1^{ij}(\boldsymbol{P})$ in (25) is lower bounded by

$$\bar{g}_1^{ij}(\boldsymbol{P}) = \sum_{h=1}^{H} B_h \log\left(\sum_{k=1}^{K} x_{k,h}p_{k,h}|\boldsymbol{g}_{i,j,h}^{\mathrm{H}}\boldsymbol{w}_{k,h}|^2+\sigma_{i,j,h}^2\right) - g_2^{ij}(\bar{\boldsymbol{P}}) - \mathrm{tr}[\nabla g_2^{ij}(\bar{\boldsymbol{P}})^{\mathrm{T}}(\boldsymbol{P}-\bar{\boldsymbol{P}})], \tag{28}$$

where $\bar{\boldsymbol{P}}=\{\bar{p}_{j,h}\}\in\mathbb{C}^{K\times H}$ is an arbitrarily given matrix with $\bar{p}_{j,h}\geqslant 0$, $g_2^{ij}(\bar{\boldsymbol{P}})$ is defined by (27), and $\nabla g_2^{ij}(\bar{\boldsymbol{P}})$ is the derivative of $g_2^{ij}(\boldsymbol{P})$ at $\bar{\boldsymbol{P}}$ with its (m,n)-th element being

$$[\nabla g_2^{ij}(\bar{\boldsymbol{P}})](m,n) = \begin{cases} 0, & \text{if } m=j, \\ \dfrac{B_n x_{m,n}|\boldsymbol{g}_{i,j,n}^{\mathrm{H}}\boldsymbol{w}_{m,n}|^2}{\sum_{k=1,k\neq j}^{K} x_{k,n}\bar{p}_{k,n}|\boldsymbol{g}_{i,j,n}^{\mathrm{H}}\boldsymbol{w}_{k,n}|^2+\sigma_{i,j,n}^2}, & \text{otherwise.} \end{cases} \tag{29}$$

Furthermore, $\bar{g}_1^{ij}(\boldsymbol{P})$ is concave with respect to $\boldsymbol{P}$, and $\bar{g}_1^{ij}(\boldsymbol{P}) = g_1^{ij}(\boldsymbol{P})$ if $\bar{\boldsymbol{P}}=\boldsymbol{P}$.

Proof: According to Lemma 1, we derive an upper bound of the concave function $g_2^{ij}(\boldsymbol{P})$ as

$$g_2^{ij}(\boldsymbol{P}) \leqslant g_2^{ij}(\bar{\boldsymbol{P}}) + \mathrm{tr}[\nabla g_2^{ij}(\bar{\boldsymbol{P}})^{\mathrm{T}}(\boldsymbol{P}-\bar{\boldsymbol{P}})], \tag{30}$$

where $\bar{\boldsymbol{P}}=\{\bar{p}_{j,h}\}$ is a given matrix, and $\nabla g_2^{ij}(\bar{\boldsymbol{P}})$ is the derivative of $g_2^{ij}(\boldsymbol{P})$ at $\bar{\boldsymbol{P}}$. Meanwhile, the equality holds in (30) if $\bar{\boldsymbol{P}}=\boldsymbol{P}$.

By using the relationship

$$[\nabla g_2^{ij}(\bar{\boldsymbol{P}})](m,n) = \frac{\partial g_2^{ij}(\bar{\boldsymbol{P}})}{\partial p_{m,n}},$$

we can obtain the expression of $\nabla g_2^{ij}(\bar{\boldsymbol{P}})$ as in (29). By combining (30) with the definition of $g_1^{ij}(\boldsymbol{P})$ in (26), it yields that $g_1^{ij}(\boldsymbol{P}) \geqslant \bar{g}_1^{ij}(\boldsymbol{P})$ with $\bar{g}_1^{ij}(\boldsymbol{P})$ defined in (28). Meanwhile, it is straightforward to see that $\bar{g}_1^{ij}(\boldsymbol{P})$ is concave, and $g_1^{ij}(\boldsymbol{P}) = \bar{g}_1^{ij}(\boldsymbol{P})$ when $\bar{\boldsymbol{P}}=\boldsymbol{P}$. ■

Replacing $g_1^{ij}(\boldsymbol{P})$ by $\bar{g}_1^{ij}(\boldsymbol{P})$ in constraint (24a) of problem $(\hat{\mathcal{F}}_p)$, we turn to solve the following approximate problem

$$(\mathcal{F}_p) \max_{\{p_{j,h}\},t} \quad t \tag{31}$$

$$\text{s.t. } \bar{g}_1^{ij}(\boldsymbol{P}) \geqslant tR_{i,j}^0,\ \forall i,\ j, \tag{31a}$$

$$\sum_{h=1}^{H}\sum_{j=1}^{K} x_{j,h}p_{j,h}\|\boldsymbol{A}_l\boldsymbol{w}_{j,h}\|^2 \leqslant P_l,\ \forall l, \tag{31b}$$

$$p_{j,h} \geqslant 0,\ \forall j,\ h, \tag{31c}$$

where $\bar{g}_1^{ij}(\boldsymbol{P})$ is defined in (28). Obviously, constraint set (31a) is a convex set, and it is a subset of constraint set (24a). Thus, problem $(\mathcal{F}_p)$ is a lowered bounded by problem $(\hat{\mathcal{F}}_p)$ in terms of the optimal objective value. We regard the optimal solution to problem $(\mathcal{F}_p)$ as the approximate solution of problem $(\hat{\mathcal{F}}_p)$. It is worth noting that, problem $(\mathcal{F}_p)$ is convex with respect to $\boldsymbol{P}$, and thereby can be easily solved by CVX toolbox [33]. Meanwhile, iteratively solving problem $(\mathcal{F}_p)$ multiple times can obtain a saddle point or a local minimum of problem $(\hat{\mathcal{F}}_p)$ with a feasible starting point [34].

Based on the above analyses, for a set of candidate beamforming vectors produced from $\boldsymbol{W}_h$ by Gaussian randomization method, the power scaling factors $p_{j,h}$ can be derived by solving problem $(\hat{\mathcal{F}}_p)$, and compute scaled beamforming vectors $\sqrt{p_{j,h}}\boldsymbol{w}_{j,h}$ as the final solution. Particularly, we can implement the Gaussian randomization method multiple times to generate multiple sets of candidate beamforming vectors, obtain corresponding power scaling factors $p_{j,h}$ for each set of candidate beamforming vectors, and select the optimal set of scaled beamforming vectors with the largest objective function value. In summary, the corresponding beamforming algorithm is shown in Algorithm 1.

Algorithm 1 Multicast Beamforming Algorithm:

Input: Initial $\bar{\boldsymbol{W}}_h^0$, initial $\bar{\boldsymbol{P}}^0$, maximum transmit power P_l of LEO l, prescribed threshold ϵ, $\rho = 0$.
Output: Beamforming vectors $\boldsymbol{w}_{j,h}$.
1: **repeat**
2: Obtain $\bar{\boldsymbol{W}}_h^{\rho+1}$ by solving problem $(\mathcal{F}_r)$ with given matrix $\bar{\boldsymbol{W}}_h^{\rho}$;
3: Let $\rho = \rho + 1$;
4: **until** The difference between objective function values of problem $(\mathcal{F}_r)$ in two steps is within ϵ.
5: Let $\boldsymbol{W}_h = \bar{\boldsymbol{W}}_h^{\rho}$.
6: **if** rank($\boldsymbol{W}_h$) =1 **then**
7: Use the eigenvalue decomposition to obtain $\boldsymbol{w}_{j,h}$.
8: **else**
9: Apply the Gaussian randomization to produce candidate beamforming $\tilde{\boldsymbol{w}}_{j,h}$ from $\boldsymbol{W}_h$.
10: **repeat**
11: Obtain $\bar{\boldsymbol{P}}^{\rho+1} = \{\bar{p}_{j,h}^{\rho+1}\}$ by solving problem $(\mathcal{F}_p)$ with given $\bar{\boldsymbol{P}}^{\rho}$;
12: Let $\rho = \rho + 1$;
13: **until** The difference between objective function values of problem $(\mathcal{F}_p)$ in two steps is within ϵ.
14: Let $\boldsymbol{P} = \bar{\boldsymbol{P}}^{\rho}$, i.e., $p_{j,h} = \bar{p}_{j,h}^{\rho}$, $\forall j, h$.
15: Compute scaled beamforming vectors $\boldsymbol{w}_{j,h} = \sqrt{p_{j,h}}\tilde{\boldsymbol{w}}_{j,h}$ as the final solution.
16: **end if**

For the proposed Algorithm 1, its computational complexity mainly relies on solving convex problem $(\mathcal{F}_r)$ and convex problem $(\mathcal{F}_p)$. For solving problem $(\mathcal{F}_r)$, there are K^2M^2+1 variables. By employing a primal-dual interior point method to solve problem $(\mathcal{F}_r)$, the computation complexity is $O((K^2M^2+1)^3\log(\epsilon_1^{-1}))$ with ϵ_1 being the accepted duality gap. Similarly, for solving convex problem $(\mathcal{F}_p)$, it involves $KH+1$ variables. By also employing a primal-dual interior point method, the corresponding computation complexity is $O((KH+1)^3\log(\epsilon_2^{-1}))$ with ϵ_2 being the accepted duality gap. Therefore, the total computational complexity of Algorithm 1 is formulated as

$$O\left(\left(K^2M^2+1\right)^3\log\left(\epsilon_1^{-1}\right)\right)+O\left(\left(KH+1\right)^3\log\left(\epsilon_2^{-1}\right)\right). \tag{32}$$

B. Subchannel Assignment Algorithm

Section IV-A has shown solving beamforming vector $\boldsymbol{w}$ with fixed subchannel assignment strategy $\boldsymbol{X}$. This subsection will show how to utilize the matching game to acquire the desirable subchannel assignment scheme $\boldsymbol{X}$.

To obtain the optimal subchannel assignment, it is straightforward to traverse all possible subchannel assignment schemes. However, it is not feasible in practice due to the high computation complexity. Nevertheless, we can formulate the binary subchannel assignment matrix $\boldsymbol{X}$ as a solution to a matching model. Particularly, one subchannel can match with several GU groups, while one GU group can occupy several subchannels. As a result, the subchannel assignment can be considered as a many-to-many matching game. On the other hand, according to the expression of the achievable rate in (9), GUs on the same subchannel will cause signal interference among them. Thus, the achievable rate of a GU is affected by not only the subchannels that are matched with, but also other GUs sharing the same subchannel. Therefore, the subchannel assignment problem is considered as a many-to-many matching game with peer effects [37], [38].

By partitioning the optimizations of subchannel assignment $\boldsymbol{X}$ and downlink beamforming $\boldsymbol{w}$, we first equivalently rewrite problem $(\mathcal{F})$ as follows

$$(\mathcal{F}_{\mathcal{X}})\ \max_{\boldsymbol{X}}\left(\max_{\boldsymbol{w}_{j,h}}\min_{j\in\{1,\ldots,K\}}\min_{i\in[1,G_j]}\frac{1}{R_{i,j}^0}R_{i,j}\right) \tag{33}$$

$$\text{s.t.}\ \sum_{h=1}^{H}\sum_{j=1}^{K}x_{j,h}\|\boldsymbol{A}_l\boldsymbol{w}_{j,h}\|^2\leqslant P_l,\ \forall l, \tag{33a}$$

$$x_{j,h}\in\{0,1\},\ \forall j,\ h, \tag{33b}$$

$$\sum_{h=1}^{H}x_{j,h}\geqslant 1,\ \forall j. \tag{33c}$$

Recall that, constraint (33c) implies that at least one subchannel should be assigned to each group.

Denoting $\mathcal{G}=\{\mathcal{G}_1,\ldots,\mathcal{G}_K\}$ as the set of K GU groups and $\mathcal{C}=\{c_1,\ldots,c_H\}$ as the set of H subchannels, let $\mathcal{C}$ and $\mathcal{G}$ be player sets of the subchannel-GU group matching game, we can view the binary subchannel assignment matrix $\boldsymbol{X}$ as a solution to this matching problem. Referring to [39], we first give the following definition for integrity and clarity.

Definition 1: A mapping μ is a many-to-many matching if $\mathcal{C}\to\mathcal{G}$ satisfies:

- for arbitrary $g\in\mathcal{G}$, $\mu(c)\subseteq\mathcal{G}$,
- for arbitrary $c\in\mathcal{C}$, $\mu(g)\subseteq\mathcal{C}$,
- $g\in\mu(c)$ only when $c\in\mu(g)$,

in which $\mu(g)$ denotes occupied subchannels by GU group g, and $\mu(c)$ is the set of GU groups on subchannel c under the matching μ.

Each group can choose multiple subchannels in $\mathcal{C}$ as the communication media, and each subchannel can match with a subset of GU groups in $\mathcal{G}$. In our setup, we aim at maximizing the system capacity. Hence, the criterion of preference list for one group is based on the received power from every subchannel. Especially, with the channel gain of $\mathcal{U}_{i,j}$ over c_h being $\boldsymbol{g}_{i,j,h}$, the lowest received power in group $\mathcal{G}_k$ over subchannel c_h is given by $\min_{i\in[1,G_j]}\|\boldsymbol{g}_{i,j,h}\boldsymbol{w}_{j,h}\|^2$. The preference list criterion for subchannel c is based on the total benefit of the system, i.e., the system capacity. That is to say, the overall system benefit is expressed as

$$\mathbf{Bft}=\min_{j\in\{1,\ldots,K\}}\min_{i\in[1,G_j]}\frac{1}{R_{i,j}^0}R_{i,j}, \tag{34}$$

where $R_{i,j}$ is calculated as (9) with involved beamforming vector $\boldsymbol{w}$ is solved by Algorithm 1. Then, when g selects c, subchannel

c will accept the selection only when the system performance, i.e., system benefit **Bft** in (34), will be enhanced.

According to [37], [38], [39], a stable solution is envisioned as the desirable solution for the mapping problem, where there are no unmatched players and all of them have a preference to become partners. However, due to the large amount of players in $\mathcal{C} \cup \mathcal{G}$, it poses difficulties in finding the stable partners for each player. Similar to [39], to characterize the stability of the solution to the subchannel-GU group matching problem, we give the definition of pair-wise stable in Definition 2, before which the following two notations are introduced. For a given $\hat{\mathcal{C}} \subseteq \mathcal{C}$, we denote $\mathcal{C}_g(\hat{\mathcal{C}}) \subseteq \hat{\mathcal{C}}$ by the set that is preferred by g to occupy; Likewise, for a given $\hat{\mathcal{G}} \subseteq \mathcal{G}$, we define $\mathcal{G}_c(\hat{\mathcal{G}}) \subseteq \hat{\mathcal{G}}$ as the set that wish to occupy c. For a GU group $g \in \mathcal{G}$, with two given subsets of $\mathcal{C}$ being Ω' and Ω'', we define $\Omega' \succ \Omega''$ as the meaning that subchannels in Ω' are more preferred than Ω'' by g; Similarly, for a subchannel $c \in \mathcal{C}$ and two subsets $\Theta', \Theta'' \subseteq \mathcal{G}$, $\Theta' \succ \Theta''$ means that c is preferred to be assigned to groups in Θ' than Θ''.

Definition 2: A matching relation μ is said to be pair-wise stable if there exists no (c, g) with $c \notin \mu(g)$ and $g \notin \mu(c)$ satisfying $\{c'\} \succ \mu(g)$ and $\{g'\} \succ \mu(c)$ for arbitrary $c' \in \mathcal{C}_g(\mu(g) \cup \{c\})$ and arbitrary $g' \in \mathcal{G}_c(\mu(c) \cup \{g\})$.

For the many-to-many matching model, the pair-wise stability is a significant property, and we thereby seek the solution with pair-wise stability [37], [38], [39]. Through letting each player (i.e., subchannel or GU group) select its partner successively one by one from the opposite set instead of a subset, we can obtain a solution with pair-wise stability [39]. Accordingly, we propose Algorithm 2 to realize choosing the partner one by one for each player.

Remark 1: For one player (GU group or subchannel), its rejected partner during a certain intermediate process is possible to be accepted in later iterations. For instance, subchannel $c \in \mathcal{C}$ is not allocated to GU group $g \in \mathcal{G}$ at the l-th iteration, but both $c \in \mu(g)$ and $g \in \mu(c)$ are possible to hold true at the l'-th ($l' > l$) iteration.

The following theorem shows the convergence property for Algorithm 2 according to [39].

Theorem 3: Algorithm 2 can reach a pair-wise stable solution to the subchannel-GU group matching problem within a finite number of iterations.

Proof: We first prove that Algorithm 2 is convergent to a pair-wise stable solution by contradiction.

We assume that the final matching μ obtained by Algorithm 2 is not pair-wise stable. Then, according to Definition 2, there exist a GU group g and a subchannel c with $c \notin \mu(g)$ and $g \notin \mu(c)$ such that both $\{c'\} \succ \mu(g)$ and $\{g'\} \succ \mu(c)$ hold true with $c' \in \mathcal{C}_g(\mu(g) \cup \{c\})$ and $g' \in \mathcal{G}_c(\mu(c) \cup \{g\})$. Since we have $\{g'\} \succ \mu(c)$, GU group g' selects subchannel c to match with in some earlier iteration. Note that, both $c \notin \mu(g)$ and $g \notin \mu(c)$ hold true. Thus, either subchannel c had some better preference compared with GU group g and rejected group g, or accepted GU group g and then made a replacement with a certain other GU group in the latter iteration at the proposal time of group g. Then, we have the relationship that $g' \notin \mathcal{C}_c(\mu(c) \cup \{g\})$, which leads to a contradiction. Hence, matching relation μ is pair-wise stable.

Algorithm 2 Subchannel Assignment Algorithm Using Many-to-Many Matching Model.

Input: Subchannel set $\mathcal{C}$, GU group set $\mathcal{G}$, $\mathcal{G}_c = \emptyset$ with $\forall c \in \mathcal{C}$, $\Omega_g = \emptyset$ with $\forall g \in \mathcal{G}$.
Output: Subchannel assignment $\boldsymbol{X}^*$.

```
Produce the preference list of GU group G_j ∈ G, i.e., {min_{i∈[1,G_j]} ||g_{i,j,h}||^2}.
for ite = 1, ..., Ite_max do
  for j = 1, ..., K do
    Represent GU group G_j as g, and let c be the optimal unassigned subchannel in preference list of g.
    Let strategy set S = ∅, S_0 = ∅, and throughput set T = ∅.
    Create a replacement strategy s: replacing g' ∈ G_c by g, and adding s to S.
    Construct an addition strategy s: inserting g to G_c, and adding s to S.
    for s ∈ S do
      Update affected subchannel set C' for strategy s.
      ∀c' ∈ C', use Algorithm 1 to solve beamforming vectors, and compute Bft by (34).
      if Bft is better than benefit of C' without implementing s then
        Add s to S_0 and insert Bft to T.
      end if
    end for
    Let s_Best = arg max_{s∈S_0} T.
    if s_Best is a replacement strategy then
      G_c = (G_c/{g'}) ∪ {g}, Ω_{g'} = Ω_{g'}/{c} and Ω_g = Ω_g ∪ {c}, that is, g' is the to-be-replaced group and g is the new group on subchannel c.
      Use Algorithm 1 to solve beamforming vectors.
      Update preference lists of g and g'.
    else
      G_c = G_c ∪ {g} and Ω_g = Ω_g ∪ {c}.
      Use Algorithm 1 to solve beamforming vectors.
      Update preference list of g.
    end if
    Terminate if s_Best is empty.
  end for
  Terminate if there is no further change in Bft.
end for
```

In the sequel, we will show that Algorithm 2 will converge in finite iterations.

First, no matter whether a minimization problem is convex or not, its global or local optimum solution admits a nature of convexity. In Algorithm 2, each accepted strategy can improve the system performance compared with the previous choices. Through addition and substitution strategies, we propose possible operations for the tagged group and its most preferred subchannel. The tagged group is added to the most preferred subchannel or replaces an existing group matched with the subchannel if and only if the system performance is improved by this operation. Hence, in each iteration, when the system

performance is improved, the process goes towards the convergence state gradually, since the solution always exists in the finite domain. ■

Based on Theorem 3, Algorithm 2 can obtain a pair-wise stable solution to the subchannel-GU group many to many mapping problem. Finally, we give the result about the computational complexity of Algorithm 2. According to [39], the outer two loops of the algorithm admit a polyhedral time complexity, which can be represented by $O(K^{c_1}H^{c_2})$ with c_1 and c_2 being constants. It is significantly less compared to the brute-force searching with the computation complexity $\mathcal{O}(2^{KH})$. Inside these loops, for a given subchannel assignment strategy, the computation complexity of computing benefit is regarded as that of Algorithm 1, which is $O((K^2M^2+1)^3\log(\epsilon_1^{-1}))+O((KH+1)^3\log(\epsilon_2^{-1}))$. Therefore, the overall computation complexity is

$$O\left(K^{c_1}H^{c_2}(K^2M^2+1)^3\log(\epsilon_1^{-1})\right) + O\left(K^{c_1}H^{c_2}(KH+1)^3\log(\epsilon_2^{-1})\right), \tag{35}$$

which implies that Algorithm 2 admits a polynomial computation complexity.

It is worth noting that, the computation of the subchannel assignment and downlink beamforming scheme by Algorithm 2 can be placed in the central controller MEO satellite. When the MEO finishes the computation process, it first conveys the obtained subchannel assignment and downlink beamforming strategy to corresponding LEO satellites. After LEO satellites received the resource scheduling signalling, each LEO transmits its multicast contents to GUs where the contents are pre-relayed via the nearest satellite Earth stations and on-board routing. Note that, due to the short latency of signalling transmission, these LEO satellites can almost synchronously receive the signalling messages and multicast contents to GUs.

V. Numerical Simulations

In the simulation section, we present numerical results to demonstrate the validity of the proposed subchannel assignment and beamforming design for multigroup multicast cooperative transmissions in ultra-dense LEO networks.

Assume that the SpaceX V-band non-geostationary orbit satellite system, consisting of two sub-constellations with a total of 11927 LEO satellites, provides downlink multicast services for GUs distributed in the west area of China. According to the SpaceX satellite constellations, during a certain time period, a total of $L=5$ LEO satellites are available to cover the western area simultaneously, and these L LEO satellites are at the height of around 1200 km. We adopt the same values for the remaining parameters of LEO satellites as presented in [27] and [30], which are listed in Table II. The LEO satellites use Ka frequency band to serve GUs with total bandwidth of B_{tol} over $H=5$ subchannels, and the total frequency band is divided into H subchannels, with each subchannel having an equal bandwidth of $B_h = B_{tol}/H$. Correspondingly, the power of the AWGN is given by $\sigma^2_{i,j,h} = B_h N_0$, where N_0 denotes the power spectral density of the AWGN. In our setup, there are overall $K=3$ contents for GUs with predefined-locations in the west area to request, and thus these GUs are divided into $K=3$ groups based on their requested contents. Meanwhile, assume each GU group has $G_k = G = 3$ GUs. Then, the total amount of GUs is $N = GK = 9$. Moreover, assume that two antennas are equipped on one LEO satellite, while the others have one antenna, resulting in a total of $M=6$ antennas. The maximum transmit power of each LEO satellite is set to $P_l = P_{\max} = 50$ dBm, $l = 1,\ldots,L$. The predetermined target achievable rate is set to $R^0_{i,j} = 1$ by default. We set other main simulation parameters as in Table II.

TABLE II
Main Simulation Parameters

Parameter	Value
Total available bandwidth for the LEO satellites B_{tol}	500 MHz
Frequency band	(Ka) 20 GHz
AWGN power spectral density N_0	-174 dBm/Hz
Power attenuation of the rain fading ξ	1
3dB angle $\theta_{3\text{dB}}$	0.2°
Threshold in Algorithms 1: ϵ	10^{-2}

To evaluate the effectiveness of the proposed approach (referred to as "SCA + Matching"), we will compare it with two benchmark approaches, which are respectively named as "MRT + Best" and "SCA + Random", respectively. For MRT + Best approach, each GU group directly picks the subchannel where the lowest received power (i.e., $\min_{i\in[1,G_j]}\|\boldsymbol{g}_{i,j,h}\|^2$) is maximized, the beamforming is obtained using the maximum ratio transmission (MRT) method [40], which can be represented as

$$\boldsymbol{w}^l_{j,h} = \sqrt{P^{\text{ave}}_{h,j}}\frac{\boldsymbol{A}^l\boldsymbol{v}_{j,h}}{\|\boldsymbol{A}^l\boldsymbol{v}_{j,h}\|}, \tag{36}$$

where $\boldsymbol{v}_{j,h} = \boldsymbol{g}_{i_0,j,h}$, $i_0 = \arg\max_i \|g_{i,j,h}\|^2$, and $P^{\text{ave}}_{h,j} = P_{\max}/(H_0\,N^h_j)$ with N^h_j representing the amount of GU groups occupying c_h, while H_0 denotes the total number of occupied subchannels. In the SCA + Random approach, the binary subchannel assignment $\boldsymbol{X}$ is generated in a random manner, and the beamforming scheme is yield using Algorithm 1 with the given random subchannel assignment matrix. Particularly, for the SCA + Random method, we randomly produce $\boldsymbol{X}$ 20 times to obtain the average system performance. Using the specified downlink beamforming and subchannel assignment, we calculate the capacity of $\mathcal{G}_j$ and the system capacity as follows:

$$C_j = \min_{i\in[1,G_j]} R_{i,j} \text{ and } C = \min_{j\in\{1,\ldots,K\}}\ \min_{i\in[1,G_j]} \frac{1}{R^0_{i,j}}R_{i,j},$$

and the maximum system capacity obtained by derived downlink beamforming and subchannel assignment of a certain method is referred to the system MMF capacity. The approach with higher system MMF capacity admits better performance.

First, we demonstrate the convergence of the proposed SCA+Matching method. Fig. 2 displays the MMF system capacity as the outer-most loop iterations increase for three scenarios of $H = \{3,4,5\}$. As shown in Fig. 2, it can be observed that, system MMF capacity increases with iterations before reaching the convergence point, and the convergence is reached in finite iterations in all cases, which is coincident with Theorem 3. We

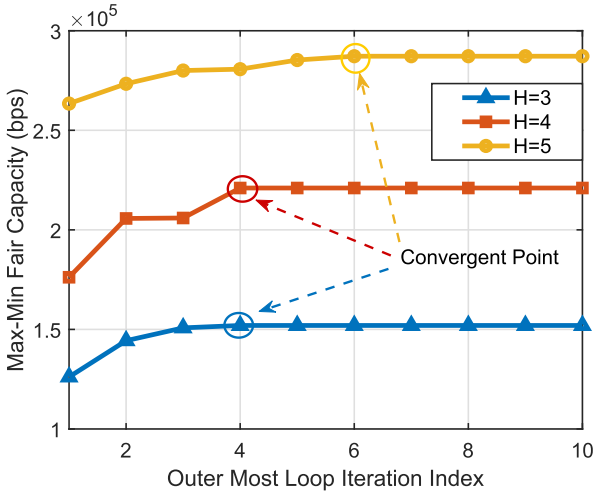

Fig. 2. Convergence results.

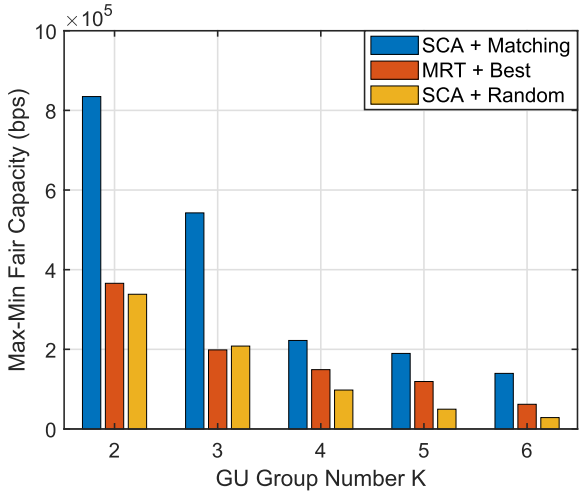

Fig. 4. System MMF capacities of different numbers of groups.

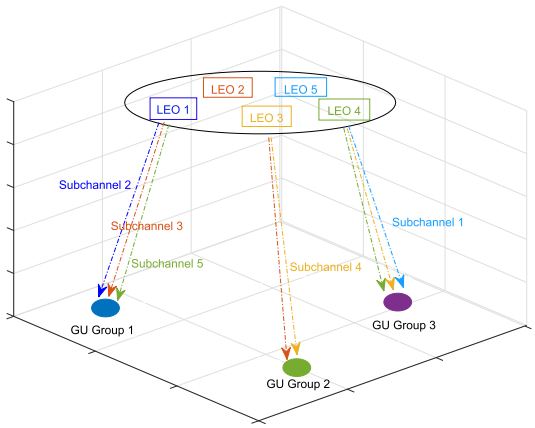

Fig. 3. Subchannel assignment diagram with $K = 3, H = 5$.

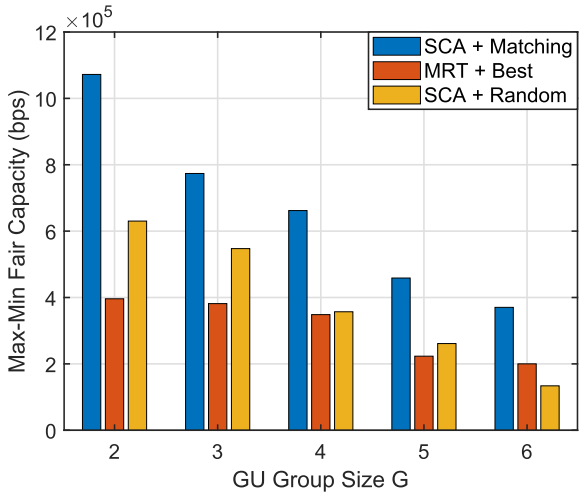

Fig. 5. System MMF capacities of different GU group sizes.

can observe that, the iteration number is nondecreasing with the increase of H. Meanwhile, Fig. 2 shows that, a larger H leads to a better system capacity, since more subchannels can reduce inter-group interferences.

The subchannel assignment for the case of $K = 3$ GU groups and $H = 5$ subchannels is shown in Fig. 3. Although GUs in one group may be distributed in different locations in practice, their subchannel assignments are the same, and thus we plot each GU group as a whole in Fig. 3 for clarification. As shown in Fig. 3, GU group 1 is served by subchannel 2, subchannel 3 and 5, GU group 2 is matched with subchannel 3 and 4, while subchannel 1, 4 and 5 are allocated to GU group 3. We can see that all subchannels are assigned uniformly, which is also coincident with the intuition.

In the sequel, we will show the effectiveness of the proposed SCA+Matching approach and how the involved parameters will affect the system MMF capacity.

1) Comparison of Different Group Number K: We evaluate the proposed SCA+Matching method for $K = \{2, 3, 4, 5, 6\}$, where other parameters are set as aforementioned. It can be observed from Fig. 4, the proposed SCA+Matching approach outperforms both MRT+Best and SCA+Random approaches. Additionally, the system MMF capacities of all approaches decrease with the increase of K. In particular, for the SCA+Matching method, when K increases from 2 to 6, the system MMF capacity decreases continuously by approximately 75%. The performance degradation is explained by an increase in inter-group interference caused by the addition of GU groups.

2) Comparison of Different Group Size G: Similarly, with the other parameters set as aforementioned, we consider different GU group size for cases of $G = \{2, 3, 4, 5, 6\}$. As shown in Fig. 5, the proposed SCA+Matching approach admits the best performance compared with MRT+Best and SCA+Random in all cases. Furthermore, in the five cases, the system MMF capacities decrease with increasing G. For the SCA+Matching method, the system MMF capacity decreases by about 64% as the GU group size varies from 2 to 6, due to inter-group interference. It can be seen that the decrease in system MMF capacity in Fig. 5 is smaller than that in Fig. 4, which is because the inter-group interference caused by increasing the GU group size is less than that caused by increasing the GU group number. Combining Figs. 4 and 5, we observe that the system performance falls rapidly when the GU number exceeds antenna number.

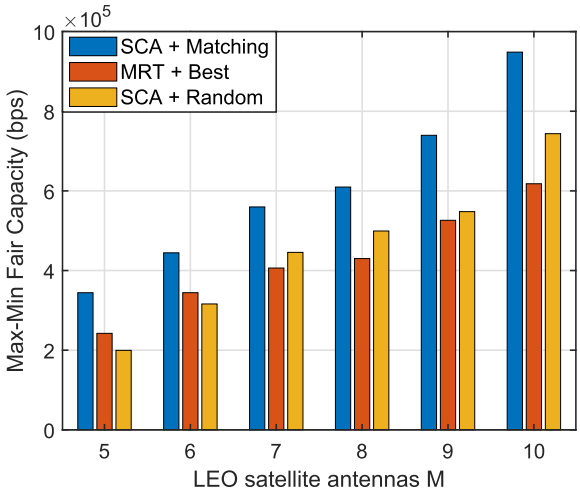

Fig. 6. System MMF capacities of different antenna numbers.

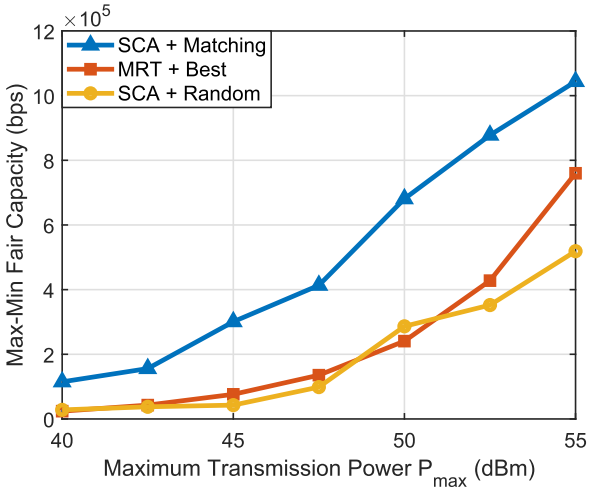

Fig. 7. System MMF capacities of different maximum transmission powers.

3) Comparison of Different LEO Satellite Antennas M: For these $L = 5$ LEO satellites simultaneously covering the west area, when the antenna number of each LEO varies from one to two, the overall antenna number M has six cases, i.e., $M = \{5, 6, 7, 8, 9, 10\}$. For these six cases, we display the system MMF capacities of all three approaches in Fig. 6, where the proposed SCA+Matching approach performs the best. With increasing antenna number M, the system MMF capacities of all approaches admit an increase trend. This is due to the fact that more LEO antennas provide more degrees of freedom, which can mitigate inter-group interference. Therefore, for a large number of GUs, a larger number of antennas should be used to achieve high system MMF capacity.

4) Comparison of Different Maximum Transmission Power $P_{\max}$: Fig. 7 presents a comparison of the system performances among the three approaches for 7 cases of $P_{\max} = \{40, 42.5, 45, 47.5, 50, 52.5, 55\}$ dBm. It can be observed that SCA+Matching performs better than the other two methods. Additionally, as $P_{\max}$ increases, all of the three methods have an increasing trend in the system MMF capacity. This is attributed to higher achievable rate of each GU for a larger $P_{\max}$, which promotes the system MMF capacity accordingly.

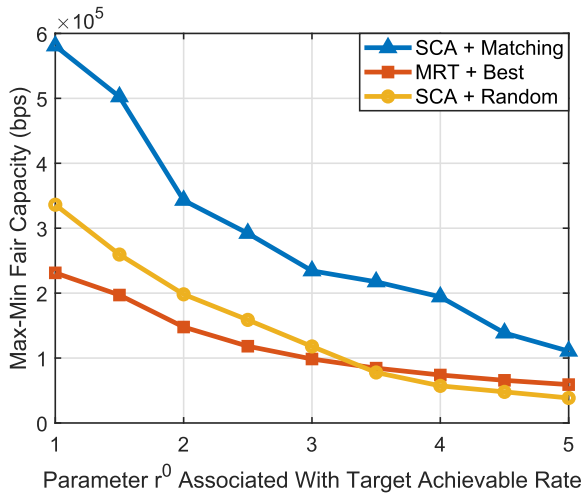

Fig. 8. Impact of target achievable rate $R^0_{i,j}$ on the system MMF capacity.

5) Comparison of Different Target Achievable Rate $R^0_{i,j}$: We consider a scenario with fixed parameters $K = 3$, $H = 5$, $M = 6$ and $G = 4$. Notably, the system MMF capacity only relies on the relative values of $R^0_{i,j}$ when other parameters are fixed. With a given number r^0, the target achievable rates of GUs are correspondingly set to: (1) For GUs in GU group 1, $R^0_{i,1} = 1$; (2) for half of the GUs in GU group 2, $R^0_{1,2} = R^0_{2,2} = 1$, and for the remaining GUs in GU group 2, $R^0_{3,2} = R^0_{4,2} = r^0$; (3) for GUs in GU group 3, $R^0_{i,3} = r^0$. In Fig. 8, we illustrate the system MMF capacities for 9 cases of parameter r^0 associated with the target achievable rate, i.e., $r^0 = \{1, 1.5, 2, 2.5, 3, 3.5, 4, 4.5, 5\}$. As can be seen, the system MMF capacity increases with r^0, and the SCA+Matching method exhibits the best system performance among these three methods. This trend coincides with the intuition, because larger r^0 leads to the fact that GUs with higher target achievable rates will occupy more resources, which will reduce the lowest achievable rate of all GUs. Since the lowest achievable rate among all GUs determines the system MMF capacity, a larger r^0 leads to a lower system MMF capacity.

In Fig. 9, we illustrate the capacity of each GU group for $r^0 = \{1, 2, 3, 4, 5\}$, where GU group 1 and GU group 3 respectively have the lowest and highest target achievable rates. As shown in Fig. 9, GU group 3 has the highest MMF capacity while GU group 1 has the lowest MMF capacity. Meanwhile, in Fig. 9, as r^0 increases, the capacities of GU group 2 and 3 increase while the capacity of GU group 1 decreases. As more resources will be allocated to the groups with a higher target achievable rate, i.e., GU group 2 and 3, the MMF capacity of GU group 1 decreases accordingly.

VI. Conclusion and Future Work

In this article, we have investigated the multigroup multicast cooperative transmissions in an ultra-dense LEO network, where GUs require different contents. To maximize the system MMF capacity, we have proposed an efficient iterative algorithm that employs the SCA and matching game technologies to jointly

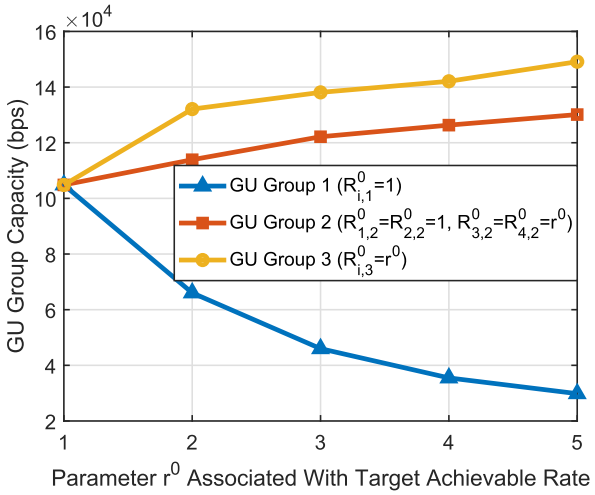

Fig. 9. Impact of target achievable rate $R^0_{i,j}$ on the group capacity.

optimize the beamforming design and subchannel assignment matrix. Simulation results have shown that the proposed method outperforms benchmark methods in terms of system MMF capacity. This work has the potential to offer valuable directives for multigroup multicast cooperative transmission in ultra-dense LEO networks. In the future work, we will consider the multigroup multicast transmissions for a space-air-ground integrated network where LEO satellites combined with terrestrial BSs and aerial platforms cooperatively provide multicast service for GUs, and we will also consider the case with imperfect CSI to reduce the impact of the propagation delay on CSI.

REFERENCES

[1] N. Kato et al., "Optimizing space-air-ground integrated networks by artificial intelligence," *IEEE Wireless Commun.*, vol. 26, no. 4, pp. 140–147, Aug. 2019.

[2] S. Fu, J. Gao, and L. Zhao, "Collaborative multi-resource allocation in terrestrial-satellite network towards 6G," *IEEE Trans. Wireless Commun.*, vol. 20, no. 11, pp. 7057–7071, Nov. 2021.

[3] T. Ma et al., "UAV-LEO integrated backbone: A ubiquitous data collection approach for B5G Internet of Remote Things networks," *IEEE J. Sel. Areas Commun.*, vol. 39, no. 11, pp. 3491–3505, Nov. 2021.

[4] T. Duan and V. Dinavahi, "Starlink space network-enhanced cyber-physical power system," *IEEE Trans. Smart Grid*, vol. 12, no. 4, pp. 3673–3675, Jul. 2021.

[5] A. Z. Yalcin, M. Yuksel, and B. Clerckx, "Rate splitting for multi-group multicasting with a common message," *IEEE Trans. Veh. Technol.*, vol. 69, no. 10, pp. 12281–12285, Oct. 2020.

[6] X. Zhu, C. Jiang, L. Yin, L. Kuang, N. Ge, and J. Lu, "Cooperative multigroup multicast transmission in integrated terrestrial-satellite networks," *IEEE J. Sel. Areas Commun.*, vol. 36, no. 5, pp. 981–992, May 2018.

[7] R. Zhang, R. Ruby, J. Pan, L. Cai, and X. Shen, "A hybrid reservation/contention-based MAC for video streaming over wireless networks," *IEEE J. Sel. Areas Commun.*, vol. 28, no. 3, pp. 389–398, Apr. 2010.

[8] B. Qian, H. Zhou, T. Ma, K. Yu, Q. Yu, and X. Shen, "Multi-operator spectrum sharing for massive IoT coexisting in 5G/B5G wireless networks," *IEEE J. Sel. Areas Commun.*, vol. 39, no. 3, pp. 881–895, Mar. 2021.

[9] M. Röper and A. Dekorsy, "Robust distributed MMSE precoding in satellite constellations for downlink transmission," in *Proc. IEEE 2nd 5G World Forum*, 2019, pp. 642–647.

[10] M. Y. Abdelsadek, H. Yanikomeroglu, and G. K. Kurt, "Future ultra-dense LEO satellite networks: A cell-free massive MIMO approach," in *Proc. IEEE Int. Conf. Commun. Workshops*, 2021, pp. 1–6.

[11] D. Goto, H. Shibayama, F. Yamashita, and T. Yamazato, "LEO-MIMO satellite systems for high capacity transmission," in *Proc. IEEE Glob. Commun. Conf.*, 2018, pp. 1–6.

[12] C. He, Q. Chen, A. Cao, J. Chen, and R. Jin, "Application of the time modulated array in satellite communications," *IEEE Wireless Commun.*, vol. 26, no. 2, pp. 24–30, Apr. 2019.

[13] Z. Xiao, L. Zhu, J. Choi, P. Xia, and X.-G. Xia, "Joint power allocation and beamforming for non-orthogonal multiple access (NOMA) in 5G millimeter wave communications," *IEEE Trans. Wireless Commun.*, vol. 17, no. 5, pp. 2961–2974, May 2018.

[14] N. Sidiropoulos, T. Davidson, and Z.-Q. Luo, "Transmit beamforming for physical-layer multicasting," *IEEE Trans. Signal Process.*, vol. 54, no. 6, pp. 2239–2251, Jun. 2006.

[15] E. Karipidis, N. D. Sidiropoulos, and Z.-Q. Luo, "Quality of service and max-min fair transmit beamforming to multiple cochannel multicast groups," *IEEE Trans. Signal Process.*, vol. 56, no. 3, pp. 1268–1279, Mar. 2008.

[16] Q.-D. Vu, K.-G. Nguyen, and M. Juntti, "Weighted max-min fairness for C-RAN multicasting under limited fronthaul constraints," *IEEE Trans. Commun.*, vol. 66, no. 4, pp. 1534–1548, Apr. 2018.

[17] M. Tao, E. Chen, H. Zhou, and W. Yu, "Content-centric sparse multicast beamforming for cache-enabled cloud RAN," *IEEE Trans. Wireless Commun.*, vol. 15, no. 9, pp. 6118–6131, Sep. 2016.

[18] G. Zhou, C. Pan, H. Ren, K. Wang, and A. Nallanathan, "Intelligent reflecting surface aided multigroup multicast MISO communication systems," *IEEE Trans. Signal Process.*, vol. 68, pp. 3236–3251, 2020.

[19] M. Sadeghi, E. Björnson, E. G. Larsson, C. Yuen, and T. L. Marzetta, "Max-min fair transmit precoding for multi-group multicasting in massive MIMO," *IEEE Trans. Wireless Commun.*, vol. 17, no. 2, pp. 1358–1373, Feb. 2018.

[20] S. He et al., "Cloud-edge coordinated processing: Low-latency multicasting transmission," *IEEE J. Sel. Areas Commun.*, vol. 37, no. 5, pp. 1144–1158, May 2019.

[21] J. Wang, L. Zhou, K. Yang, X. Wang, and Y. Liu, "Multicast precoding for multigateway multibeam satellite systems with feeder link interference," *IEEE Trans. Wireless Commun.*, vol. 18, no. 3, pp. 1637–1650, Mar. 2019.

[22] V. Joroughi, M. A. Vázquez, and A. I. Pérez-Neira, "Generalized multicast multibeam precoding for satellite communications," *IEEE Trans. Wireless Commun.*, vol. 16, no. 2, pp. 952–966, Feb. 2017.

[23] L. You, A. Liu, W. Wang, and X. Gao, "Outage constrained robust multigroup multicast beamforming for multi-beam satellite communication systems," *IEEE Wireless Commun. Lett.*, vol. 8, no. 2, pp. 352–355, Apr. 2019.

[24] Digital Video Broadcasting (DVB), *Second Generation Framing Structure, Channel Coding and Modulation Systems for Broadcasting, Interactive Services, News Gathering and Other Broadband Satellite Applications; Part 2: DVB-S2 Extensions (DVB-S2X)*, European Standard EN 302 307-2, European Telecommunications Standards Institute, Sophia Antipolis, France, Oct. 2014.

[25] 3GPP, "Study on architecture for next generation system," 3rd Generation Partnership Project (3GPP), Tech. Rep. 23.799 V14.0.0, Dec. 2016.

[26] G. Araniti, I. Bisio, M. D. Sanctis, A. Orsino, and J. Cosmas, "Multimedia content delivery for emerging 5G-satellite networks," *IEEE Trans. Broadcast.*, vol. 62, no. 1, pp. 10–23, Mar. 2016.

[27] G. Zheng, S. Chatzinotas, and B. Ottersten, "Generic optimization of linear precoding in multibeam satellite systems," *IEEE Trans. Wireless Commun.*, vol. 11, no. 6, pp. 2308–2320, Jun. 2012.

[28] Y. Li et al., "A novel two-layered optical satellite network of LEO/MEO with zero phase factor," *Sci. China Inf. Sci.s*, vol. 53, no. 6, pp. 1261–1276, Jun. 2010.

[29] C. Liu, W. Feng, Y. Chen, C.-X. Wang, and N. Ge, "Optimal beamforming for hybrid satellite terrestrial networks with nonlinear PA and imperfect CSIT," *IEEE Wireless Commun. Lett.*, vol. 9, no. 3, pp. 276–280, Mar. 2020.

[30] D. Christopoulos, S. Chatzinotas, and B. Ottersten, "Multicast multigroup precoding and user scheduling for frame-based satellite communications," *IEEE Trans. Wireless Commun.*, vol. 14, no. 9, pp. 4695–4707, Sep. 2015.

[31] C. Liu, W. Feng, Y. Chen, C.-X. Wang, and N. Ge, "Optimal beamforming for hybrid satellite terrestrial networks with nonlinear PA and imperfect CSIT," *IEEE Wireless Commun. Lett.*, vol. 9, no. 3, pp. 276–280, Mar. 2020.

[32] D. P. Bertsekas, *Nonlinear Programming*. Belmont, MA, USA: Athena Scientific, 1999.

[33] M. Grant and S. Boyd, "CVX: MATLAB software for disciplined convex programming, version 2.1," Mar. 2014. [Online]. Available: http://cvxr.com/cvx

[34] M. Hast, K. J. Astrom, B. Bernhardsson, and S. Boyd, "PID design by convex-concave optimization," in *Proc. Eur. Control Conf.*, 2013, pp. 4460–4465.

[35] L. Zhou, "QoE-driven delay announcement for cloud mobile media," *IEEE Trans. Circuits Syst. Video Technol.*, vol. 27, no. 1, pp. 84–94, Jan. 2017.
[36] L. Zhou, "Mobile device-to-device video distribution: Theory and application," *ACM Trans. Multimedia Comput. Commun. Appl.*, vol. 12, no. 3, pp. 1–23, Mar. 2016.
[37] Y. Gu, W. Saad, M. Bennis, M. Debbah, and Z. Han, "Matching theory for future wireless networks: Fundamentals and applications," *IEEE Commun. Mag.*, vol. 53, no. 5, pp. 52–59, May 2015.
[38] A. E. Roth, "Stability and polarization of interests in job matching," *Econometrica*, vol. 52, no. 1, pp. 47–57, Jan. 1984.
[39] R. Ruby, S. Zhong, H. Yang, and K. Wu, "Enhanced uplink resource allocation in non-orthogonal multiple access systems," *IEEE Trans. Wireless Commun.*, vol. 17, no. 3, pp. 1432–1444, Mar. 2018.
[40] Z. Wang, Y. Cao, D. Zhang, X. Hua, P. Gao, and T. Jiang, "User selection for MIMO downlink with digital and hybrid maximum ratio transmission," *IEEE Trans. Veh. Technol.*, vol. 70, no. 10, pp. 11101–11105, Oct. 2021.

Ting Ma (Member, IEEE) received the B.S., M.S., and Ph.D. degrees in statistics from Sichuan University, Chengdu, China, in 2013, 2016, and 2020, respectively. She is currently a Postdoctoral Fellow with the School of Electronic Science and Engineering, Nanjing University, Nanjing, China. Her research interests mainly include space-air-ground integrated networks, convex optimization theory, robust hypothesis testing and game theory.

Bo Qian (Member, IEEE) received the B.S. and M.S. degrees in statistics from Sichuan University, Chengdu, China, in 2015 and 2018, respectively, and the Ph.D. degree in information and communication engineering from Nanjing University, Nanjing, China, in 2022. He is currently a Postdoctoral Fellow with Peng Cheng Laboratory, Shenzhen, China. His research interests include resource management in B5G/6 G networks, VANET, network economics, blockchain, and game theory. He was the recipient of the Best Paper Award from IEEE VTC-Fall 2020.

Xiaohan Qin (Student Member, IEEE) received the B.S. degree in communication engineering from Central South University, Changsha, China, in 2020. She is currently working toward the Ph.D. degree in communications and information system with Nanjing University, Nanjing, China. Her research interests include space-air-ground integrated networks, network resource management, and game theory.

Xin Zhang (Graduate Student Member, IEEE) received the B.S. degree in mathematics and physics basic science from the University of Electronic Science and Technology of China, Chengdu, China, in 2020. She is currently working toward the Ph.D. degree in communications and information system with Nanjing University, Nanjing, China. Her research interests include space-air-ground integrated netowrks, resource allocation, and convex optimization theory.

Lin X. Cai (Senior Member, IEEE) received the M.A.Sc. and Ph.D. degrees in electrical and computer engineering from the University of Waterloo, Waterloo, ON, Canada, in 2005 and 2010, respectively. She is currently an Associate Professor with the Department of Electrical and Computer Engineering, Illinois Institute of Technology, Chicago, IL, USA. Her research interests include green communication and networking, intelligent radio resource management, and wireless Internet of Things. She was the recipient of the Postdoctoral Fellowship Award from the Natural Sciences and Engineering Research Council of Canada in 2010, Best Paper Award from the IEEE GLOBECOM 2011, NSF Career Award in 2016, and the IIT Sigma Xi Research Award in the Junior Faculty Division in 2019. She is an Executive Editorial Committee Member of IEEE TRANSACTION ON WIRELESS COMMUNICATIONS, an Associate Editor for IEEE TRANSACTION ON VEHICULAR TECHNOLOGIES, and the Co-Chair for IEEE Conferences.

Haibo Zhou (Senior Member, IEEE) received the Ph.D. degree in information and communication engineering from Shanghai Jiao Tong University, Shanghai, China, in 2014. From 2014 to 2017, he was a Postdoctoral Fellow with the Broadband Communications Research Group, Department of Electrical and Computer Engineering, University of Waterloo, Waterloo, ON, Canada. He is currently a Full Professor with the School of Electronic Science and Engineering, Nanjing University, Nanjing, China. His research interests include resource management and protocol design in B5G/6G networks, vehicular ad hoc networks, and space-air-ground integrated networks. He was the recipient of the 2019 IEEE ComSoc Asia-Pacific Outstanding Young Researcher Award. He was selected as an IEEE ComSoc Distinguished Lecturer for the class during 2023–2024. He was the Track/Symposium CoChair for IEEE/CIC ICCC 2019, IEEE VTC-Fall 2020, IEEE VTC-Fall 2021, and IEEE GLOBECOM 2022. He is currently an Associate Editor for IEEE TRANSACTIONS ON WIRELESS COMMUNICATIONS, IEEE INTERNET OF THINGS JOURNAL, *IEEE Network Magazine,* and IEEE WIRELESS COMMUNICATIONS LETTER.